Phase-Gated Amplitude Connectivity: A Dimension-Preserving Fusion of PCC and PLV for EEG-Based Cognitive-state Classification

Yuzeng Xu
Graduate School of Schience and Engineering, Chiba University
Chiba, Japan
yuzeng-xu@chiba-u.jp

Sho Otsuka
Center for Frontier Medical Engineering, Chiba University
Chiba, Japan
Otsuka.s@chiba-u.jp

Seiji Nakagawa
Center for Frontier Medical Engineering, Chiba University
Chiba, Japan
s-nakagawa@chiba-u.jp

***Abstract*—Functional connectivity derived from electroencephalography (EEG) has become one of the commonly used feature representations in brain–computer interface (BCI) systems. Among available measures, the Pearson correlation coefficient (PCC) and phase locking value (PLV) are widely used and often fused because they provide complementary information: PCC captures amplitude-based coupling in the time domain, whereas PLV reflects phase-based synchronization in the frequency domain. Existing fusion strategies typically rely on heuristic embedding schemes, such as additive, multiplicative, or structural splicing operations. However, most existing fusion approaches are primarily engineering-driven, relying on heuristic rules or generic concatenation strategies, with limited consideration of the distinct signal-level characteristics between amplitude- and phase-based connectivity measures in EEG brain network analysis. To address this limitation, we propose a fusion strategy guided by the complementary properties of these measures, termed Phase-Gated Amplitude Connectivity (PG-AC). The proposed method treats PCC as the primary amplitude-based representation and uses PLV as a reliability-aware gating mechanism to selectively modulate PCC connections and suppress noise-driven or spurious couplings. Experimental results on EEG-based cognitive-state classification demonstrated that the proposed method consistently outperforms PCC-only, PLV-only, and commonly used fusion strategies, including additive, multiplicative and splicing-based approaches.**

Keywords—EEG, brain-computer interface, functional connectivity, feature fusion, cognitive computing, deep learning

I. INTRODUCTION

With the rapid development of neuroscience and machine learning, it has become increasingly feasible to recognize human cognitive activities by following a structured processing pipeline, ranging from neural signal acquisition and feature engineering to downstream classification tasks.

Electroencephalography (EEG) is one of the most classical and widely adopted modalities for quantifying human brain activity, as it records the microvolt-level electrical potential generated by neuronal populations. Despite the emergence of modern neuroimaging techniques such as magnetoencephalography (MEG), functional MRI, and functional near-infrared spectroscopy (NIRS), EEG remains one of the most practical measurement tools in contemporary brain–computer interface (BCI) research and applications [1]. This is largely due to its non-invasive nature, high temporal resolution, and low cost.

Functional connectivity characterizes the statistical dependency among EEG channels and reflects interactions among brain regions or neuronal assemblies at a network level. In neuroscience, functional connectivity has been extensively employed to reveal large-scale brain organization and inter-regional communication [2]. More recently, its dynamic representations have attracted growing attention in BCI engineering, where functional connectivity patterns serve as discriminative and learnable features that encode cognitive processes for machine learning–based systems [3], [4].

Several approaches have been proposed for estimating functional connectivity from EEG signals. Among them, the Pearson correlation coefficient (PCC) is one of the most commonly used measures, as it quantifies the linear amplitude correlation between pairs of channels in the time domain. Phase-based metrics, such as the phase locking value (PLV) and the phase lag index, characterize phase synchronization and phase-lead relationships between signals and are widely employed to capture oscillatory interactions in the frequency domain. Directional connectivity measures, including transfer entropy and Granger causality, further extend functional connectivity analysis by modeling directed information flow between neural signals.

Despite the availability of diverse connectivity estimators, PCC and PLV remain the most frequently adopted features in dynamic functional connectivity analysis and EEG-based cognitive classification tasks, owing to their broad applicability and relatively low computational cost [2]. These two measures provide complementary descriptions of brain interactions, capturing amplitude-based coupling in the time-domain and phase-based synchronization in the frequency domain, respectively.

To jointly exploit time-domain and phase-based characteristics, several studies have explored fusion strategies that combine PCC- and PLV-derived connectivity patterns. A commonly adopted approach is feature stacking, in which multiple functional connectivity matrices (e.g., PCC and PLV) are treated as parallel feature channels or concatenated representations and jointly fed into downstream classifiers such as convolutional neural networks (CNNs) [5]. However, stack-based fusion inevitably increases feature dimensionality and model complexity, resulting in higher computational cost and memory consumption. Such drawbacks are particularly critical for practical BCI applications, where real-time responsiveness, limited computational resources, and energy efficiency are key constraints.

In this context, fusion strategies that preserve input dimensionality deserve careful consideration. Dimension-preserving fusion schemes aim to integrate heterogeneous connectivity information into a single functional matrix without expanding the data size, thereby offering a more

deployment-oriented balance between information richness and computational efficiency. Representative approaches include constructing a fused functional matrix, in which multiple connectivity estimators are embedded into a unified 2D representation and subsequently processed by CNNs—for example, pairwise fusion across PCC, PLV, mutual information, and transfer entropy, with PCC+PLV serving as a typical configuration [6]. Related implementations also exploit the inherent structural properties of functional connectivity matrices, such as symmetry, by assigning different estimators to complementary matrix regions (e.g., upper versus lower triangular parts [7]). These structure-preserving fusion strategies maintain the original input size while injecting heterogeneous coupling information, enabling efficient multimodal integration without dimensional expansion.

However, most existing fusion approaches are engineering-driven, relying on heuristic rules or simple concatenation, with little consideration of the distinct signal-level characteristics of amplitude- and phase-based EEG connectivity measures. To address this, we propose Phase-Gated Amplitude Connectivity (PG-AC), a fusion strategy that exploits their complementary properties. PG-AC treats PCC as the primary amplitude-based representation and uses PLV as a reliability-aware gate to modulate PCC connections and suppress spurious couplings.

Experiments on EEG-based cognitive-state classification show that PG-AC consistently outperforms PCC-only, PLV-only, and common fusion methods, including additive, multiplicative, and splicing-based approaches.

II. Method

A. Feature Engineering

Preprocessing consisted of 50 Hz low-pass filtering to suppress electromagnetic interference and electromyographic noise, followed by average re-referencing. The EEG signals were decomposed into five canonical frequency bands (delta, theta, alpha, beta, and gamma), of which the alpha, beta, and gamma bands were selected for feature extraction due to their stronger association with emotional processing [8]. Feature engineering involved segmenting the EEG signals into non-overlapping 1-s windows, followed by the computation of functional connectivity using PCC and PLV.

For time series such as EEG signals, PCC quantifies the linear relationship between two signals of x_{ci} and x_{cj}, which is defined as:

$$PCC(x_{ci}, x_{cj}) = \frac{\sum_{t=1}^{T}(x_{ci,t}-\overline{x_{ci}})(x_{cj,t}-\overline{x_{cj}})}{\sqrt{\sum_{t=1}^{T}(x_{ci,t}-\overline{x_{ci}})^2}\sqrt{\sum_{t=1}^{T}(x_{cj,t}-\overline{x_{cj}})^2}}, \quad (1)$$

where $\overline{x_{ci}}, \overline{x_{cj}}$ are the respective means, and T denotes the total number of samples.

PLV measures the phase synchronization strength between two signals across time:

$$PLV(x_{ci}, x_{cj}) = \left| \frac{1}{T}\sum_{t=1}^{T} e^{j(\phi_{x_{ci}}(t)-\phi_{x_{cj}}(t))} \right| \quad (2)$$

where $\phi_{x_{ci}}(t)$ and $\phi_{x_{cj}}(t)$ are the instantaneous phases of the two signals, $j = \sqrt{-1}$.

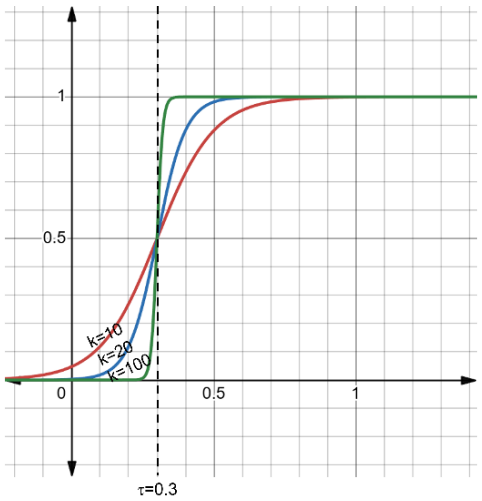

Fig. 1. Illustration of the sigmoid gating function with different steepness parameters k and a fixed threshold τ (=0.3). Increasing k yields a sharper transition, approaching hard-gating behavior.

B. Proposed Method for Feature Fusion

Linear amplitude correlations in the time-domain, such as PCC, are generally regarded as informative and capable of capturing rich interaction details; however, they are also susceptible to various sources of noise, most notably contamination induced by volume conduction. In contrast, phase-based synchronization measures such as PLV are less sensitive to such artifacts and can effectively suppress spurious zero-lag correlations, but may simultaneously discard potentially meaningful amplitude-related information. Motivated by the complementary characteristics of these functional connectivity measures, this study proposes a novel feature fusion method, which is the PG-AC.

Specifically, PCC-based functional matrix is adopted as the primary representation, while a PLV-derived function is constructed to serve as a gating criterion for identifying and suppressing noise-driven or unreliable connections in the PCC matrix. Through this mechanism, amplitude-based connectivity information is selectively retained or attenuated under the guidance of phase synchrony. As a result, a fused functional matrix is obtained. Importantly, the proposed method preserves the original feature dimensionality, yielding a representation equivalent in size to a conventional PCC- or PLV-based connectivity matrix, while embedding heterogeneous coupling characteristics in a structured and physiologically informed manner.

The fused functional connectivity *FFC* and proposed feature fusion are defined as:

$$FFC(x_{ci}, x_{cj}) = \alpha \cdot PCC(x_{ci}, x_{cj}), \quad (3)$$

$$\alpha(x_{ci}, x_{cj}) = \frac{1}{1+\exp(-k\cdot(PLV(x_{ci},x_{cj})-\tau))}, \quad (4)$$

where α denotes the sigmoid gating function that modulates the PCC magnitude according to the reliability information provided by PLV, also shown in Fig. 4. The sigmoid parameter $\tau \in [0,1]$ defines the gating threshold, consistent with the range of PLV, while k controls the steepness of the gating response.

The parameter τ determines the PLV threshold at which PCC connections begin to be reliably retained, while k

controls the sharpness of the gating transition. As shown in Fig. 1 larger values of k lead to a steeper sigmoid function, enabling a more decisive separation between low-PLV (potentially noise-driven) and high-PLV (reliable) connections.

C. Competing Methods

To evaluate the effectiveness of the proposed PG-AC, functional matrices constructed using original PCC and original PLV individually are included as baseline methods. In addition, three conventional feature fusion strategies are employed: multiplicative fusion, additive fusion (normalize PCC to [0,1] at first), and splicing fusion, in which different connectivity features are inserted into the upper and lower triangles of a single functional connectivity matrix. In total, six functional connectivity representations are evaluated, including the proposed PG-AC method.

D. Dataset and Data Partitioning

Method evaluation was conducted on the SJTU Emotion EEG Dataset (SEED) [8], a widely used benchmark in emotion recognition research. The dataset contains 62-channel EEG recordings (international 10–20 system) from 15 subjects, each participating in three independent experiments, yielding a total of 45 experiment recordings. In each experiment, subjects watched 15 pre-labeled video clips (approximately 4 minutes each) designed to elicit emotions with three valence categories: negative (–1), neutral (0), and positive (+1). Recordings annotated with corresponding valence labels.

The dataset (15 subjects × 3 experiments with EEG recordings) was divided into two non-overlapping subsets: a single development subset comprising 5 subjects (5 × 3 recordings) and an evaluation subset comprising 10 subjects (10 × 3 recordings). The subset with 5 subjects was used for parameter optimization and for subsequent constructing the node-retention list, which was subsequently used for subnetwork extraction. The subset with 10 subjects (10 × 3 recordings) was used for downstream classification experiments.

E. Subnetwork Extraction

When using full-scale functional matrices, performance differences among methods may be marginal, as all representations contain sufficient discriminative information and thus tend to achieve similarly high classification accuracy. To enable a more discriminative comparison, subnetwork extraction was performed based on node retention, using node retention lists derived from average node strength.

Specifically, nodes were ranked according to their average node strength, computed across all functional connectivity matrices in the development subset, and the top nodes, determined by the node retention rate (NRR), were retained to construct subnetworks that served as classification samples.

As described in the data-partitioning section, node-retention lists were constructed exclusively on the development subset, which was strictly isolated from downstream classification experiments. Although both parameter optimization and node-retention list construction were performed on the same subset without further subdivision, the node-retention lists were derived after model optimization and were based on the corresponding optimal models. Node retention lists differed across methods, as node strength rankings were computed independently for each connectivity representation.

F. Deep Learning Architecture and Experiment Settings

All six functional connectivity representations—namely, the original PCC and PLV matrices, additive fusion, multiplicative fusion, splicing fusion, and the proposed PG-AC—were evaluated.

All classification experiments followed an experiment-independent evaluation protocol. Specifically, within each experiment, training and testing were performed using data from the same EEG recording, without mixing data across different experiments or subjects. Consequently, for each combination of method and subnetwork size, classification was performed independently on each recording using a 5-fold cross-validation scheme. Under this setting, classification performance was summarized by reporting the mean accuracy and standard deviation across the 30 recordings (10 × 3 recordings) for each method and NRR.

A minimalist CNN was designed to perform the classification experiments in this study in order to ensure training stability, minimize the influence of extraneous variables, and avoid introducing unintended biases.

The input to the CNN is organized as N samples × B feature-channels × nC × nC, where N denotes the number of functional matrix samples derived from N seconds EEG with non-overlapping 1-s windows, $B = 3$ corresponds to the alpha, beta, and gamma frequency bands, C is the number of EEG channels, and n represents the NRR.

TABLE I
CNN ARCHITECTURE

Stage	Operation	Details
Input	Input	Functional matrices (N×B×nC×nC)
Conv Layer 1	Conv+BN+ReLU	3×3, 32 filters, stride=1, padding=1
Pooling 1	Max Pooling	3×3, stride=3
Conv Layer 2	Conv+BN+ReLU	3×3, 64 filters, stride=1, padding=1
Pooling 2	Adaptive Max Pooling	Output size=1×1(Global pooling)
Flatten	Flatten	Convert to 1D vector (64)
FC Layer 1	Fully Connected	32 neurons
FC Layer 2	Fully Connected	3 neurons
Output	SoftMax	3-category classification

III. RESULTS

A. Parameter Optmization

For construction of PG-AC, two free parameters—the sigmoid steepness parameter k and the gating threshold τ in (3) and (4), were optimized via a grid-search procedure on the isolated development subset. Average classification accuracy obtained from actual classification experiments was used as the optimization criterion. The parameters were varied within the ranges τ in {0.2, 0.3, 0.5} and k in {10, 20, 80, 100}, while the node-retention rate NRR was considered at four levels {0.1, 0.2, 0.3, 0.5}.

For each parameter combination, the model was first instantiated, after which the node-retention list was derived from the development subset under that configuration. Classification used for parameter optimization was conducted on the same development subset, without further subdivision.

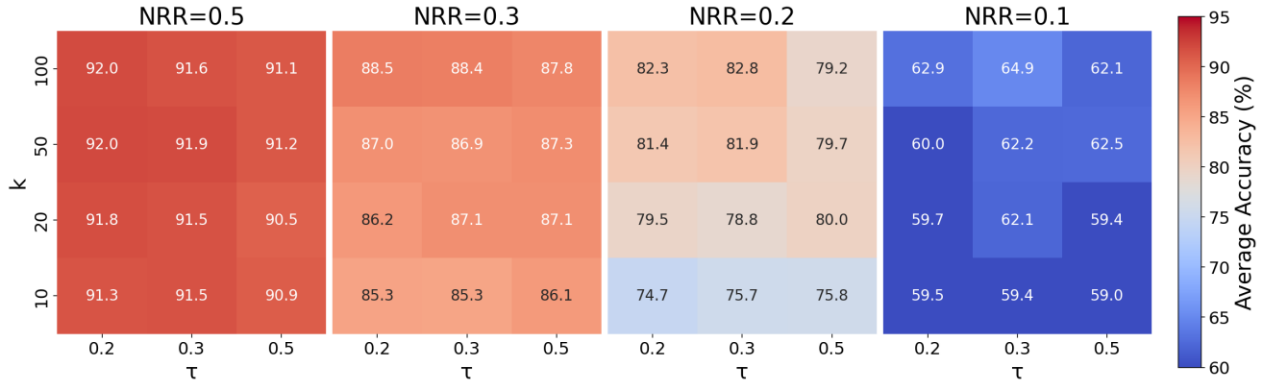

Fig. 2. Grid-search results showing the average classification accuracy (%) for each parameter configuration and NRR.

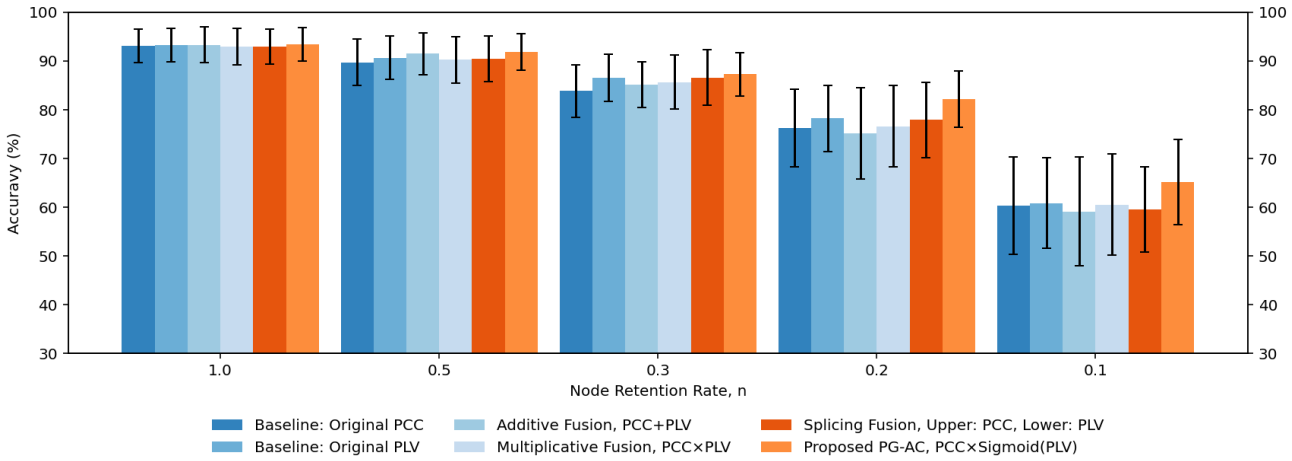

Fig. 3. Classification performances (average accuracy) for each method at different NRR values.

For each combination of parameter configurations and NRR, classification was conducted independently on each recording, and the results were then averaged across recordings. Fig. 2 illustrates the grid-search results in the form of heatmaps, reporting the mean classification accuracy for each parameter configuration and NRR.

From the grid-search results in Fig. 2, it can be observed that τ = 0.3 consistently yields superior or near-optimal classification accuracy across different NRR settings, indicating a favorable balance between suppressing spurious zero-lag correlations and preserving informative amplitude-based connectivity. In contrast, smaller or larger values of τ either retain excessive noisy connections or overly attenuate meaningful ones.

Regarding the steepness parameter, k = 100 achieves the highest or most stable performance across all evaluated selection rates. This suggests that a sharp gating mechanism is beneficial, as it enforces a clear distinction between reliable and unreliable connections rather than a gradual attenuation.

Although the parameter k can in principle be set to values larger than 100, further increasing k only makes the sigmoid gating function steeper and increasingly close to a hard cut-off. Since k = 100 already represents a sufficiently large value that yields a near-binary gating behavior, extending the search beyond this point provides negligible additional benefit. Therefore, the grid search was manually terminated at k = 100.

Based on both quantitative performance and physiological interpretability, the parameters were fixed at τ = 0.3 and k = 100 for all subsequent experiments.

B. *Classification Performance*

The average classification accuracy across recordings, for each method and NRR, was used to evaluate the performance of the methods, as reported in Table II and Fig. 3.

TABLE II
CLASSIFICATION PERFORMANCE (AVERAGE ACCURACY %) OF DIFFERENT METHODS ACROSS NRRS

Method	NRR				
	1	0.5	0.3	0.2	0.1
PCC	93.1	89.72	83.86	76.24	60.4
PLV	93.27	90.62	86.6	78.22	60.85
Additive	93.32	91.5	85.14	75.15	59.13
Multi.	93.03	90.23	85.68	76.6	60.53
Splicing	92.96	90.47	86.6	77.9	59.57
PG-AC	93.37	91.87	87.3	82.19	65.21

Overall, classification performance decreases as the functional matrix size becomes smaller. At the full size (NRR = 1), all methods—including the baseline PCC and PLV representations—achieve similarly high accuracy (93% level).

When the size is reduced to NRRs of 0.5 and 0.3, noticeable performance differences emerge: the proposed method and the additive fusion method achieve the highest accuracies; original PLV, multiplicative fusion, and splicing fusion form the second tier; while original PCC exhibits the lowest performance.

As the NRRs are further reduced to 0.2 and 0.1, the competing fusion methods (additive, multiplicative, and splicing) show substantial performance degradation, even

performing worse than one of their constituent features (original PLV). In contrast, the proposed method consistently achieves the highest accuracy and demonstrates an advantage over both baseline and competing methods. Specifically, at NRR = 0.2, the proposed method attains an average accuracy of 82.19%, which is 3.97% higher than the second-best method. Even under the extremely sparse condition of NRR = 0.1, it maintains an average accuracy of 65.21%, exceeding the second-best method by 4.36%.

C. Repeated Measures Analysis of Variance

To further examine the performance improvements achieved by the proposed method, a repeated-measures analysis of variance (RM-ANOVA) was conducted. The analysis was performed across 30 EEG recordings, with method and NRR treated as two within-subject factors. Each recording was evaluated under all method–NRR combinations. The RM-ANOVA results are summarized in Table III.

TABLE III
REPEATED ANOVA OF DIFFERENT METHODS ACROSS NRRS

	F value	Pr > F	Num DF	Den DF
Method	10.4	1.52e-8	5	145
NRR	372.73	3.39e-65	4	116
Method × NRR	5.22	3.47e-12	20	580

The RM ANOVA revealed a highly significant main effect of NRR was observed (F = 372.73; p = 3.39e-65), suggesting a strong influence of NRR levels on the results. A significant main effect of method (F = 10.40; p = 1.52e-8), indicating that performance differed significantly across the evaluated methods was also observed. Importantly, the method × NRR interaction was significant (F = 5.22; p = 3.47e-12), demonstrating that the relative performance of the methods varied across different NRR conditions.

Based on the confirmed significance of the method factor, paired t-tests and mean accuracy differences were further conducted at fixed NRRs of 0.5, 0.3, 0.2, and 0.1 to investigate whether specific performance improvements existed between the proposed method and the baseline and competing approaches. The results are presented in the spliced matrix shown in Fig. 4, where mean accuracy differences are reported in the upper triangular matrix and corresponding p-values are shown in the lower triangular matrix.

Pairwise comparisons indicate that the proposed PG-AC method exhibits statistically significant performance differences compared with all baseline and fusion methods across most comparisons ($p < 0.05$, $p < 0.005$, and $p < 0.001$) for all NRR settings. As sparsity increases from moderate conditions (NRR = 0.5, 0.3) to extremely sparse regimes (NRR = 0.2, 0.1), these significance patterns become more consistent, accompanied by larger mean difference gains achieved by PG-AC. Notably, at NRR = 0.1, all competing methods deteriorate to a comparable performance level, approaching that of the original PCC and PLV baselines. In contrast, the proposed PG-AC further widens the performance gap, highlighting its superior robustness under extreme sparsification.

Overall, the strong and consistent significance associated with PG-AC confirms that its performance gains are not confined to a specific retention regime but persist across sparsification levels. Overall, these results corroborate the accuracy trends observed in Fig. 3 and provide statistical

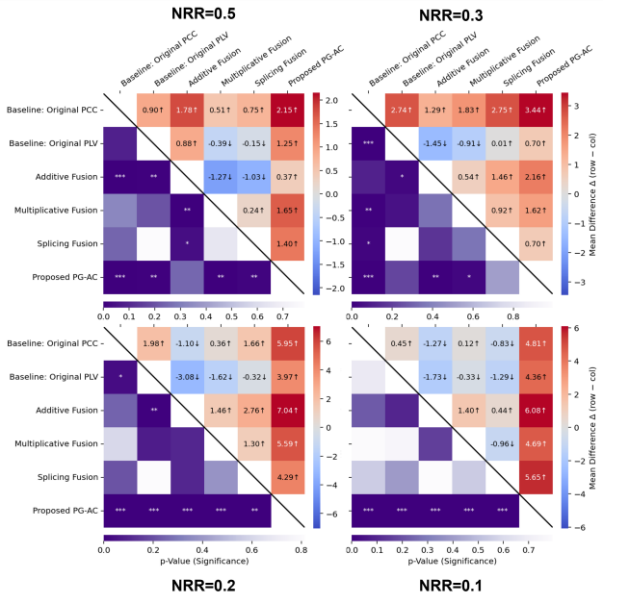

Fig. 4. Spliced matrices at different NRR values showing the mean accuracy differences (%) and p-values from paired t-test (*p<0.05, **p<0.01, ***p<0.005).

evidence that the proposed method yields a fundamentally different and more stable functional matrix organization under channel-budget constraints.

IV. DISCUSSION

Across all NRR, the proposed PG-AC method consistently demonstrated superior classification performance and statistical robustness, confirming its effectiveness in constructing discriminative functional matrices under channel-budget constraints. Notably, the performance advantage of PG-AC became increasingly pronounced as the functional matrix was sparsified, indicating that the proposed gating-based fusion produces functional representations with higher information density and improved stability for subnetwork extraction. These observations are further supported by the results of RM-ANOVA and pair-wise comparisons, which reveal significant main and interaction effects favoring PG-AC across varying NRR conditions.

In contrast, the original PCC and PLV matrices exhibited distinct but limited strengths. PCC showed competitive performance when a large number of nodes were retained, reflecting its sensitivity to amplitude-based correlations, whereas PLV demonstrated relatively higher robustness under aggressive pruning due to its insensitivity to amplitude fluctuations. However, neither metric alone was sufficient to maintain stable performance across all sparsification regimes, highlighting the need for joint modeling of amplitude and phase information.

Simple fusion strategies, including additive fusion and splicing fusion, yielded comparatively weaker and less consistent results. Additive fusion tends to amplify redundant or spatially diffuse connections without altering the underlying functional organization, which becomes detrimental when the functional matrix is aggressively reduced. Splicing fusion, while preserving heterogeneous feature roles, imposes a fixed structural partition that lacks adaptivity to node removal and fails to accommodate changes in functional topology induced by sparsification. These

limitations explain their inferior performance relative to PG-AC, particularly at low node-retention rates.

Multiplicative fusion is the closest approach to the PG-AC in terms of design philosophy. It can be regarded as a linear scaling of PCC based on PLV, where the amplitude of the primary representation (PCC) is modulated by the PLV value. In this sense, PLV serves as a credibility factor, analogous to the role it plays in PG-AC. However, multiplicative fusion lacks a gating mechanism such as the sigmoid function and does not incorporate an explicit threshold like the parameter τ used in PG-AC.

The resulting performance gap between multiplicative fusion and PG-AC suggests that critical effects emerge either during the transition from a linear transformation to a sigmoid-based nonlinearity, or from the introduction of an explicit threshold.

Further evidence is provided by the parameter optimization analysis. The functional representations consistently improve as the gating function becomes steeper, even reaching the upper bound of k=100 in our grid search. This observation supports interpreting the mechanism as an approximate hard cutoff: the full amplitude-based feature representation is preserved when the phase gate exceeds a threshold, while it is entirely discarded when the gate falls below it. In this context, the sigmoid function can be replaced by hard cutoff or multi-stage cutoff in future work. Importantly, recognizing this cutoff behavior highlights the critical role of the phase-feature threshold itself. This insight suggests that it is feasible to apply a phase-based threshold to identify and eliminate ineffective connections without introducing additional scaling coefficients to retain their information, particularly in cases where such connections are overwhelmingly more useless than useful.

V. Conclusion

This study presents a practical and effective framework for integrating amplitude- and phase-based information through a nonlinear gating mechanism. The proposed PG-AC method constructs functional matrices with higher information density and improved robustness under channel-budget constraints. Extensive experiments across varying NRRs, together with statistical analyses, demonstrate that PG-AC consistently outperforms conventional connectivity measures and fusion strategies, particularly in sparse subnetwork regimes. These results suggest that gating-based functional modeling offers a scalable and integrable solution for practical EEG-based BCI applications, where stability, interpretability, and computational efficiency are critical.

Acknowledgment

This work was supported by JSPS KAKENHI Grant Number JP24K03260 for SN and JST SPRING Grant Number JPMJSP2109 for YX.

References

[1] F. Lotte *et al.*, “A review of classification algorithms for EEG-based brain–computer interfaces: a 10 year update,” *J. Neural Eng.*, vol. 15, no. 3, p. 031005, Jun. 2018, doi: 10.1088/1741-2552/aab2f2.

[2] A. A. Fingelkurts, A. A. Fingelkurts, and S. Kähkönen, “Functional connectivity in the brain—is it an elusive concept?,” *Neuroscience & Biobehavioral Reviews*, vol. 28, no. 8, pp. 827–836, Jan. 2005, doi: 10.1016/j.neubiorev.2004.10.009.

[3] A. A. Ioannides, “Dynamic functional connectivity,” *Current Opinion in Neurobiology*, vol. 17, no. 2, pp. 161–170, Apr. 2007, doi: 10.1016/j.conb.2007.03.008.

[4] M. Hamedi, S.-H. Salleh, and A. M. Noor, “Electroencephalographic Motor Imagery Brain Connectivity Analysis for BCI: A Review,” *Neural Computation*, vol. 28, no. 6, pp. 999–1041, Jun. 2016, doi: 10.1162/NECO_a_00838.

[5] M. Wu, R. Ouyang, C. Zhou, Z. Sun, F. Li, and P. Li, “A study on the combination of functional connection features and Riemannian manifold in EEG emotion recognition,” *Front. Neurosci.*, vol. 17, Jan. 2024, doi: 10.3389/fnins.2023.1345770.

[6] E. Ahmadi Moghadam, F. Abedinzadeh Torghabeh, S. A. Hosseini, and M. H. Moattar, “Improved ADHD Diagnosis Using EEG Connectivity and Deep Learning through Combining Pearson Correlation Coefficient and Phase-Locking Value,” *Neuroinform*, vol. 22, no. 4, pp. 521–537, Oct. 2024, doi: 10.1007/s12021-024-09685-3.

[7] M. A. H. Akhand, M. A. Maria, M. A. S. Kamal, and K. Murase, “Improved EEG-based emotion recognition through information enhancement in connectivity feature map,” *Scientific Reports*, vol. 13, no. 1, p. 13804, 2023.

[8] W.-L. Zheng and B.-L. Lu, “Investigating critical frequency bands and channels for EEG-based emotion recognition with deep neural networks,” *IEEE Transactions on autonomous mental development*, vol. 7, no. 3, pp. 162–175, 2015.